# Supplemental Information for "Elastocapillary bending of microfibers around liquid droplets"

Rafael D. Schulman,[a] Amir Porat,[b] Kathleen Charlesworth,[a] Adam Fortais,[a] Thomas Salez,[bc] Elie Raphaël,[b] and Kari Dalnoki-Veress*[ab]

## S1 Analysis of Contact Region and Microfiber Shape

To analyze the wetting region between the droplet and the fiber, we begin by thresholding the image to black and white in MATLAB. The bounds of the wetting region are inputted manually, and subsequently, the contour of this region is detected. As such, we can extract the arc length of the contact region $\ell$. For several fiber radii, we plot the data for $\ell$ as a function of droplet radius in Fig. S1(a). A solid line passing through the origin is drawn alongside the data. The line describes the low-$R$ data very well, demonstrating that the empirical scaling $\ell \propto R$ in the low-$\phi$ limit is valid. The data begins to deviate from this scaling when $\phi \gtrsim 15°$.

To validate our assumption that $d \propto r$, we measure the length of the meniscus region from the images for several fiber radii with $R$ held roughly constant. The results of this analysis are displayed in Fig. S1(b), which shows that $d$ increases with $r$. A solid line passing through the origin is drawn to show that the data is consistent with the assumed scaling $d \propto r$. For a given fiber, $d$ is not found to depend on $R$.

We may also fit the central part of this wetting region to a circle to extract $R_\mathrm{f}$. In these fits, we exclude the region nearest to where the fiber exits contact with the liquid, as the fiber in this region is observed to be changing curvature towards becoming straight. A sample fit is shown in Fig. S2, where the blue region corresponds to the contour detected through image analysis, and the red circle is the fit to that data. We see that the central region of the fiber assumes a curvature of $R_\mathrm{f} > R$.

## S2 Energetic Considerations of the Winding Criterion

As outlined by Roman and Bico[1], the winding threshold can be predicted from simple energetic considerations. The transition can be explained considering a two-state model where a fiber and a droplet are either in isolation or in the wound state. Upon winding, the surface energy of the system is reduced due to contact between the droplet and the fiber by an amount $-2\gamma\beta r$ per unit length, where $\beta$ is a prefactor which depends on the details of the wetting geometry. Note that since we are in the regime $r << R$, the droplet remains nearly spherical after being wound, and any change in surface energy due to a global change in shape of the droplet is neglible (as will be demonstrated in the next section). The energetic penalty associated with winding around the droplet is an increase in bending

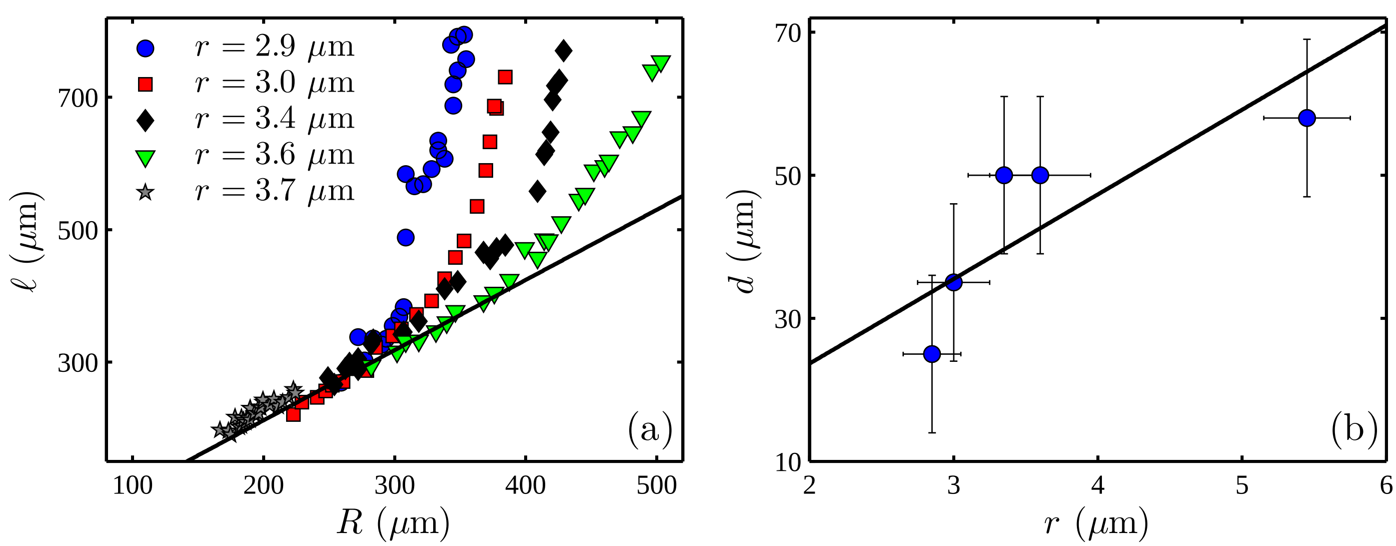


**Fig. S1** (a) The arc length of the wetted contact region between droplet and fiber as a function of droplet radius. The solid line is a straight line passing through the origin to demonstrate that $\ell \propto R$ is valid in the initial regime. (b) The meniscus size as a function of fiber radius. The solid line is a straight line passing through the origin to demonstrate that $d \propto r$ is consistent with the data.

[a] Department of Physics and Astronomy, McMaster University, 1280 Main St. W., Hamilton, ON, L8S 4M1, Canada. E-mail: dalnoki@mcmaster.ca
[b] Laboratoire de Physico-Chimie Théorique, UMR CNRS Gulliver 7083, ESPCI Paris, PSL Research University, 75005 Paris, France.
[c] Global Station for Soft Matter, Global Institution for Collaborative Research and Education, Hokkaido University, Sapporo, Hokkaido 060-0808, Japan.

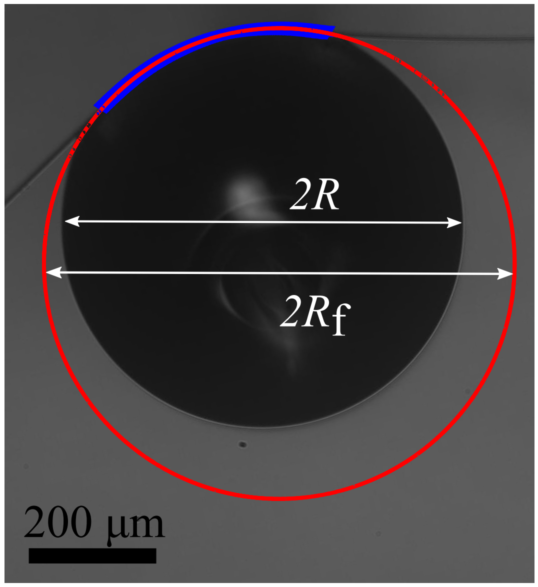


**Fig. S2** A fiber being deformed by a droplet. The contour of the central region of the fiber in contact with the droplet is detected through image analysis (blue) and fit to a circle (red circle).

energy of the fiber given by $B/2R^2$ per unit length, where $B = \pi E r^4/4$ is the bending modulus of the fiber. Thus, the total energy change upon winding is:

$$\Delta E = -2\gamma\beta r + \frac{\pi E r^4}{8R^2} \ . \tag{S1}$$

Winding occurs when it lowers the free energy of the system, which results in the winding criterion:

$$R > \alpha L_{\mathrm{BC}} \ , \tag{S2}$$

where $\alpha = \sqrt{\pi/16\beta}$. To attain a prediction for $\beta$, we must consider the microscopic wetting geometry between the fiber and the droplet. Since $r << R$, we describe the droplet as an infinite bath and the equilibrium wetting is attained in the same way as a cylinder on the surface of a liquid bath, where the liquid surface is flat and Young's law is satisfied. Overall, there is a loss of liquid-vapour and solid-vapour interface in favour of a gain of solid-liquid interface. Considering this microscopic picture, we find $\beta = \sin\theta_y + (\pi - \theta_y)\cos\theta_y$, where $\theta_y$ is the Young's angle of the liquid on the solid.

As explained in the main manuscript, for SIS we make the qualitative observation that the bending cost of the fiber not in contact with the droplet is roughly equal in magnitude to the bending cost of the fiber being wet by the droplet. Thus, the bending cost upon winding is now twice as large $\frac{\pi E r^4}{4R^2}$ whereas the gain in surface energy, $-2\gamma\beta r$, is unchanged. Ensuring a reduction in the total energy upon winding now yields $\alpha = \sqrt{\pi/8\beta}$.

## S3 Global Surface Energy Change Upon Winding

When considering the free-energy change upon the fiber winding the droplet, we only considered bending energy and wetting energy between the fiber and the droplet. In doing so, we ignored any global changes in area as the droplet assumes a lenticular shape. To justify this assumption, we must first examine the resultant lenticular shape which is depicted in Fig. S3 but was first discussed in [1]. As seen in Fig. S3(a), if we denote the radius of the initial droplet as $R_0$, then the radius at the equator of the lens will be denoted $R$, where in general $R > R_0$ to conserve volume. The radius of curvature of the spherical caps composing the lens will be denoted $R_{\mathrm{L}}$. In Fig. S3(b), we draw the microscopic picture of the wetting between the liquid and the fiber in the wound state. The circular shape of the beam is maintained as a result of a distribution of capillary forces: contact line forces $\gamma$ and Laplace pressure $P_{\mathrm{L}}$. Young's angle is satisfied between the solid and the liquid.

### S3.1 The Lens Configuration

The lens configuration can be described through a force balance on the fiber. The net liquid force acting inwards per unit length is:

$$F_{\mathrm{net},\gamma} = 2\gamma\sin\psi - \frac{2\gamma}{R_{\mathrm{L}}}\left(2r\sin(\psi+\theta_y)\right) \ , \tag{S3}$$

where $\psi$ is denoted in Fig. S3. We can use the spherical cap identity $R/R_{\mathrm{L}} = \cos\psi$ to get:

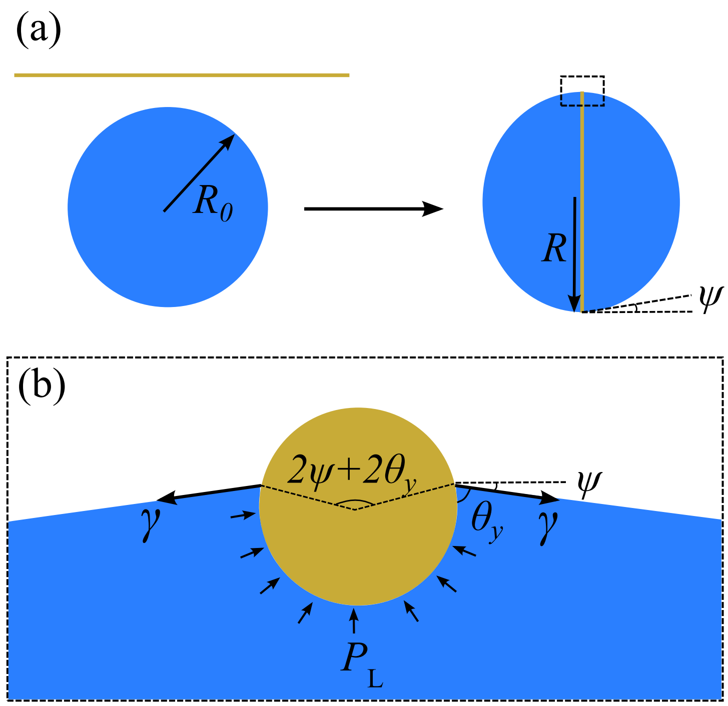


**Fig. S3** (a) A droplet of initial size $R_0$ becomes a lens of equatorial radius $R$ upon being wound by a fiber. The lens is composed of two spherical caps which intersect the equator at an angle $\pi/2-\psi$. (b) A zoomed-in cross-sectional view of the dashed rectangular area in (a). $P_L$ denotes the Laplace pressure and $\gamma$ indicates contact line surface tension forces.

$$F_{\mathrm{net},\gamma} = 2\gamma\sin\psi - \frac{4\gamma r}{R}\left(\cos\psi\sin(\psi+\theta_y)\right) . \tag{S4}$$

To maintain a circular beam, the net force per unit length acting radially inwards must be $3B_{\mathrm{rod}}/R^3$ [2]. Thus, the lens configuration must satisfy:

$$\frac{3\pi E r^4}{4R^3} = 2\gamma\sin\psi - \frac{4\gamma r}{R}\left(\cos\psi\sin(\psi+\theta_y)\right) . \tag{S5}$$

In our experiments, we observe that the lens configuration appears almost completely spherical, i.e. $\psi << 1$. Thus, to proceed further, we make the assumption $\psi << 1$, and will soon show that this is valid in our case. To first order, Eq. (S6) becomes:

$$\frac{3\pi E r^4}{4R^3} \approx 2\gamma\psi - \frac{4\gamma r}{R}\left(\psi\cos\theta_y + \sin\theta_y\right) . \tag{S6}$$

We can now isolate for $\psi$ to arrive at:

$$\psi \approx \frac{r}{R}\,\frac{\frac{3\pi L_{BC}^2}{8R^2} + 2\sin\theta_y}{1-\frac{2r}{R}\cos\theta_y} \propto \frac{r}{R} . \tag{S7}$$

Therefore, we see that $\psi$ scales as $r/R$. Since $r << R$ in our experiments and $L_{BC}/R$ is on the order of unity, $\psi << 1$ is a valid assumption.

### S3.2 Volume Conservation

Now we consider the global change in area of a droplet becoming a lens, as depicted in Fig. S3(a). We will limit our discussion to $\psi << 1$. To conserve volume, it follows that $R$ will only be slightly larger than $R_0$, i.e. $R = R_0(1+\delta)$, where $\delta << 1$. Thus, the statement of volume conservation from a spherical droplet to the two spherical caps composing the lens reads:

$$\frac{4}{3}\pi R_0^3 = \frac{2}{3}\pi\left(\frac{R}{\cos\psi}\right)^3\left(2-3\sin\psi+\sin^3\psi\right) . \tag{S8}$$

If we expand the right-hand side to second-order in $\delta$ and $\psi$ we find $\delta \approx \psi/2$.

### S3.3 Change in Area

The change in area ($\Delta\mathscr{A}$) of the droplet can be written as:

$$\Delta\mathscr{A} = 2\pi R^2 \left(1 + \tan^2\left(\frac{\pi/2 - \psi}{2}\right)\right) - 4\pi R_0^2 . \tag{S9}$$

We expand $\Delta\mathscr{A}$ to second-order in $\psi$ and $\delta$, because as we will see, the first-order term will vanish:

$$\Delta\mathscr{A} \approx 2\pi R_0^2 (1+\delta)^2 (2 - 2\psi + 2\psi^2) - 4\pi R_0^2 \tag{S10}$$

$$\Delta\mathscr{A} \approx 4\pi R_0^2 (1 + 2\delta - \psi + \psi^2 - 2\delta\psi + \delta^2) - 4\pi R_0^2 . \tag{S11}$$

The zeroth-order terms cancel, and inserting $\delta \approx \psi/2$, we find the first-order terms vanish as well, and we are left with:

$$\Delta\mathscr{A} \approx \pi R_0^2 \psi^2 = \pi \left(\frac{R}{1+\delta}\right)^2 \psi^2 \approx \pi R^2 \psi^2 , \tag{S12}$$

up to second-order in $\psi$. Since we know that $\psi \propto r/R$, we see that $\Delta\mathscr{A} \propto R^2 (r/R)^2 \sim r^2$. Therefore the change in surface energy from global area changes is $\Delta E_{\mathscr{A}} \sim \gamma r^2$. However, the change in surface energy due to wetting is $\Delta E_{\mathrm{w}} = -2\gamma r \beta (2\pi R) \sim rR$ for one complete wind, where $\beta$ depends on the microscopic wetting picture and is of order unity. Since $r << R$, we see that $\Delta E_{\mathrm{w}} \sim rR >> \Delta E_{\mathscr{A}} \sim r^2$, and we can neglect any global changes in area.

## References


1 B. Roman and J. Bico, *J. Phys. Condens. Matter*, 2010, **22**, 493101.

2 L. Landau and E. Lifshitz, *Theory of Elasticity, 3rd*, Pergamon Press, Oxford, 1986.